Solid State Phenomena
ISSN: 1662-9779, Vol. 387, pp 131-141
doi:10.4028/p-j6M0hN

Submitted: 2026-01-19
Revised: 2026-02-16
Accepted: 2026-02-17
Online: 2026-04-14

The First European Benchmark Exercise on Squeeze Flow Testing of High-Performance C-SMCs: Review

Connie Qian[1,a*], Miro Duhovic[2,b*], Louis Schreyer[3,c], Marcel Olma[3,d], Andreas Gebhard[2,e], Wouter Grouve[4,f], Dominic Schommer[2,g], Florian Gortner[2,h], Thomas Neumeyer[2,i], Luise Kärger[3,j], Martin Hohberg[5,k], Hao Yuan[6,l], Anna Julia Imbsweiler[7,m], Leah Senn Ramirez[7,n], Sepehr Simaafrookhteh[8,o], Jan Ivens[8,p], Stepan V. Lomov[8,q], Gerben Bieleman[4,9,r], Francois Mahé[10,s], Christophe Binetruy[11,t], Andreas Kapshammer[12,u], Zoltan Major[12,v], Dmitry S. Ivanov[13,w], Jonathan P.-H. Belnoue[13,x], Anatoly Koptelov[13,y], Jakub Jakimow[13,z], Yvonne Aitomaki[14,aa], Dimitra Ramantani[14,bb]

[1]School of MAC, University of Sheffield, Sheffield S1 4DT, United Kingdom

[2]Leibniz-Institut für Verbundwerkstoffe, 67663 Kaiserslautern, Germany

[3]Karlsruhe Institute of Technology, 76131 Karlsruhe, Germany

[4]Production Technology, University of Twente, 7522 NB Enschede, the Netherlands

[5]SIMUTENCE GmbH, 76131 Karlsruhe, Germany

[6]WMG, University of Warwick, Coventry CV4 7AL, United Kingdom

[7]Technical University of Munich, 85748 Garching, Germany

[8]Department of Materials Engineering, KU Leuven, 44 3001 Leuven, Belgium

[9]ThermoPlastic composites Research Center (TPRC), 7521 PN Enschede, the Netherlands

[10]Arts et Métiers Institute of Technology, LAMPA, HESAM Université, F-49035 Angers, France

[11]Nantes Université, Ecolé Centrale de Nantes, 44000 Nantes, France

[12]Institute of Polymer Product Engineering, Johannes Kepler University Linz, Linz, 4040, Austria

[13]Bristol Composites Institute, University of Bristol, Bristol BS8 1TR, United Kingdom

[14]RISE Research Institutes of Sweden, Materials and Production, Sweden

[a]c.qian@sheffield.ac.uk, [b]Miro.Duhovic@ivw.uni-kl.de, [c]louis.schreyer@kit.edu, [d]marcel.olma@kit.edu, [e]Andreas.Gebhard@ivw.uni-kl.de, [f]w.j.b.grouve@utwente.nl, [g]Dominic.Schommer@ivw.uni-kl.de, [h]Florian.Gortner@ivw.uni-kl.de, [i]Thomas.Neumeyer@ivw.uni-kl.de, [j]luise.kaerger@kit.edu, [k]martin.hohberg@simutence.de, [l]hao.yuan@warwick.ac.uk, [m]anna.julia.imbsweiler@tum.de, [n]leah.senn@tum.de, [o]sepehr.simaafrookhteh@kuleuven.be, [p]jan.ivens@kuleuven.be, [q]stepan.lomov@kuleuven.be, [r]g.bieleman@utwente.nl, [s]francois.mahe@ensam.eu, [t]christophe.binetruy@ec-nantes.fr, [u]andreas.kapshammer@jku.at, [v]zoltan.major@jku.at, [w]dmitry.ivanov@bristol.ac.uk, [x]jonathan.belnoue@bristol.ac.uk, [y]anatoly.koptelov@bristol.ac.uk, [z]jakub.jakimow@bristol.ac.uk, [aa]yvonne.aitomaki@ri.se, [bb]dimitra.ramantani@ri.se (*corresponding author)

Keywords: C-SMC, squeeze flow testing, compression moulding, benchmark exercise

Abstract. Squeeze-flow testing is a commonly used experimental method for characterising the flow behaviour of high-performance C-SMCs under typical compression moulding conditions. A European benchmark exercise involving 14 research institutions is currently being conducted to identify the sources of variability in squeeze flow testing results and to support the development of a standardised testing methodology. Experimental testing of five C-SMC materials has been completed using a well-defined testing procedure. This paper focuses on the data processing stage of the benchmark exercise, in which experimental data collected from all participants are processed and

analysed to extract information on raw material variability, force–gap height relationships, and flow-front profiles. Quantitative assessment of these results is used to identify the critical sources of variability, which subsequently informs a more detailed statistical analysis.

Introduction

High-performance carbon fibre sheet moulding compounds (C-SMCs) are a type of discontinuous fibre reinforced composite material characterised by long carbon fibre reinforcement (typically 25 mm roving length) and high fibre content (greater than 40wt%). C-SMCs can be compression moulded under high pressure (typically greater than 100 bar) to form parts with complex geometries and excellent mechanical performance. Understanding the flow behaviour of C-SMCs is key for accurately predicting manufacturing outcomes. Several research institutions have adopted squeeze flow testing for characterising the flow behaviour of SMCs [1-5], but due to the lack of a standardised testing procedure, and the unique and complex flow behaviour of high-performance SMCs, the reliability and repeatability of this testing method remain low.

The high variability observed in SMC squeeze-flow testing can be attributed to several factors. First, the raw material (material prior to processing) itself is inherently stochastic. The compounding process introduces local variations in fibre volume fraction, fibre tow size (due to filamentation), and fibre orientation, particularly during the fibre deposition stage. In addition, for thermosetting SMCs, the matrix system consists of a pre-mixed resin and hardener that has been B-staged, requiring strict control of temperature and humidity during transport, storage, and handling to minimise premature curing. These requirements are especially demanding for modern SMCs containing fast-curing resin systems, as even subtle changes in storage temperature or humidity can lead to significant variations in the degree of cure of the matrix. These, in turn, affect the matrix viscosity at processing temperatures and consequently influences the flow behaviour of the SMC.

The variation in testing equipment used also contributes to the observed variability in several ways. Squeeze flow testing is typically performed on a load frame or press with either a static or hydraulic drive, and differences in drive type can lead to variations in the accuracy of speed and position control. The choices of sensors and measurement approaches for force and displacement are other important consideration, with factors such as measurement range, linearity, and sensor location all influencing the measured results. The heating method is another significant source of variability, because the type and layout of the heating system can strongly affect the temperature distribution within the test specimen. For SMC specimens with fast-curing matrix systems, non-uniform heating can result in inhomogeneous curing and lead to variations in viscosity throughout the specimen. Finally, loss of platen parallelism is a well-known source of error in squeeze flow testing, particularly for heterogeneous materials such as SMC, as it can lead to asymmetrical pressure distributions during the test.

The actual testing procedure is another area in which large differences among research institutes are commonly observed in the literature. Unlike factors such as fibre architecture, the environmental history of the raw material, and the testing equipment, variations in the testing procedure is often strongly influenced by researchers' interpretations of representative processing conditions. The affected parameters include for example specimen size, number of layers, testing speed, specimen loading time and the tooling surface conditions.

A benchmark exercise on squeeze flow testing of C-SMCs is currently being conducted by a consortium of European research institutions with in-house squeeze flow testing facilities. The primary objective of this exercise is to identify the sources of variability in experimentally measured data and to investigate ways to improve the reliability and repeatability of the testing. A previous paper, presented at ESAFORM 2025 [6] summarised the experimental methodologies adopted in the benchmark, with a focus on the materials, testing facilities, and testing procedures. The present paper focuses on the data-processing methodology required to enable comparison of results across all participants. Based on initial observations of the processed data, a strategy for detailed quantitative analysis is proposed to establish statistical and physical correlations among variables in the experimental methodology and the measured results.

Experimental Methodology

The benchmark exercise involves 14 participating institutions across Europe, operating a total of 10 squeeze flow testing facilities. Participating institutions include École Centrale de Nantes (ECN) and HESAM Université (HESAM), Leibniz-Institut für Verbundwerkstoffe (IVW), Johannes Kepler University Linz (JKU), Karlsruhe Institute of Technology (KIT) and Simutence GmbH (SIM), KU Leuven (KUL), the University of Twente (UTW) and the ThermoPlastic Composites Research Center (TPRC), RISE Research Institutes of Sweden AB (RISE), the Technical University of Munich (TUM), the University of Bristol (UOB), Warwick Manufacturing Group (WMG), and the University of Sheffield (UOS).

Five vinyl ester (VE) based C-SMC materials (Table 1) are investigated in this benchmark exercise to examine the effects of fibre content and tow size on the flow behaviour of C-SMCs. All materials studied contain the same resin system, featuring a specialised formulation that allows the material to remain processable for up to 12 weeks when stored at room temperature (up to 23 °C). The long shelf life at room temperature is expected to reduce material variability arising from large, unpredictable environmental fluctuations, since controlling temperature variations at room temperature is considerably easier than maintaining frozen conditions. All materials were kept in sealed packaging with the original protective films during transport and storage to mitigate humidity fluctuations and evaporation loss of low molecular weight resin components. In addition, temperature and humidity sensors were kept with the material at all times to record any variations in storage conditions among the different participants.

Table 1. Summary of the materials tested in the first European C-SMC squeeze flow benchmark exercise [6].

Product code	Fibre tow size	Fibre length [mm]	Fibre weight fraction [%]	Target areal weight [g/m^2]
24 CF50-50K	50K	25.4	50	1800
24 CF50-12K	12K	25.4	50	1800
24 CF50-3K	3K	25.4	50	1800
24 CF40-12K	12K	25.4	40	1800
24 CF60-12K	12K	25.4	60	1800

A well-defined experimental procedure was implemented to mitigate the contribution of procedural variation to results variability. All test specimens were square-shaped and consisted of six plies laid up in a consistent orientation (in relation to the roll direction). Two different specimen sizes were investigated, with edge lengths of 50 mm and 100 mm. Depending on the size of testing equipment available, participants tested either both specimen sizes or only the 50 mm specimens. Specific guidance, including time limits for specimen cutting and lay-up, was provided to all participants to minimise the duration for which raw material was exposed to ambient conditions.

All testing was performed using an open-cavity, constant-mass configuration, as shown in Figure 1, with a constant mould surface temperature of 140 °C. To minimise variation in boundary conditions across participants, all testing surfaces were lined with polyimide films coated with each participant's choice of release agent. A specimen loading time of 10 s was imposed to reduce variability in preheating time, which could otherwise lead to significant differences in the initial degree of cure between tests. All tests started at an initial cavity height of 11 mm and ended at final cavity heights of 7 mm, 5 mm, or 3 mm. Each specimen was then cured for a minimum of 210 s before being removed from the testing surface. Six repeats were performed for each testing and specimen configuration, with the test order fully randomised to eliminate systematic drift associated with material aging and time-dependent variations in operator or machine behaviour. The detailed experimental methodology can be found in the previous paper [6].

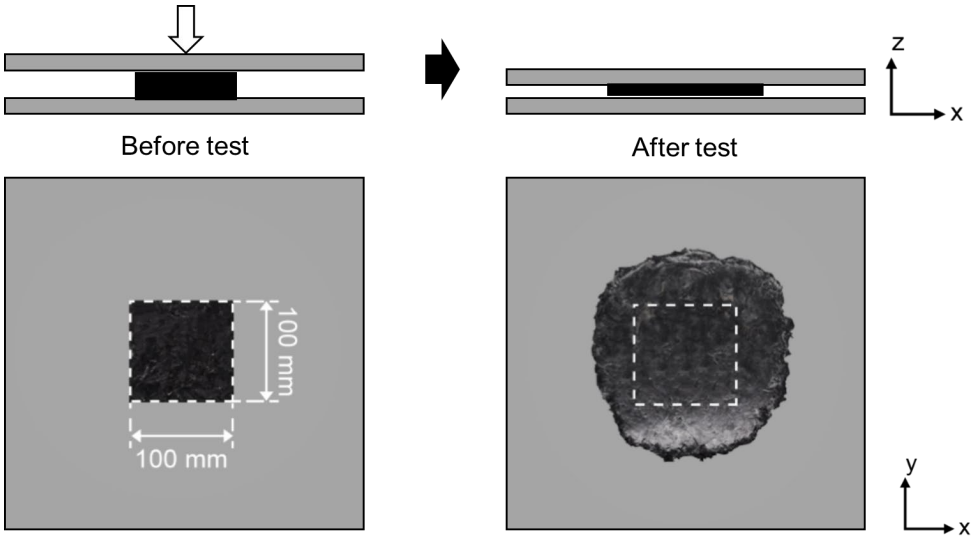

Fig. 1. Schematic illustration of the C-SMC squeeze flow test [6].

Data Processing Methodology

Following the completion of the testing campaign, four sets of raw data were collected from each participant, including testing information, unprocessed force-displacement or force-gap height data for each specimen, scanned plan view images of the specimens after testing and temperature-humidity history data for the materials from raw material production to final pressing. Information of specimens prior to testing, including thickness, density and areal weight, were used to investigate material variability. The force–displacement or force-gap height data were further processed and plotted using an in-house Python-based program developed by KIT to enable visual comparison across all participants, as well as a subsequent statistical analysis. The specimen images were processed using an in-house Python-based program developed by IVW to extract the flow front profiles for further analysis. Both data processing programs were centrally developed and executed to avoid errors and discrepancies that could arise if data processing were performed independently by individual participants.

The following sections describe the data processing methodology, starting with the weight and thickness of the raw specimens, followed by the force–gap height curves, and finally the flow-front profiles that were extracted from the specimen images.

Variability in raw material. The material variability was assessed from the thickness, density and areal weight data for raw specimens collected from all participants. Prior to each test, participants were required to measure the weight and thickness of the specimen. The density and areal weight were subsequently calculated based on the nominal specimen size.

Force-gap height relationship. The unprocessed force-displacement or force-gap height data were collected from each participant as machine-readable files. Participants who recorded both displacement and gap height data were asked to identify which measurement they considered to be more reliable and should therefore be selected for downstream data processing and analysis. A separate comparison study was performed to examine differences between the two datasets; however, details of this study are not discussed in the present paper.

The unprocessed data were imported and processed as follows. First, the data-reading function mapped the material type, specimen size (50 mm or 100 mm), and final gap height (7 mm, 5 mm, or 3 mm) according to each participant's testing plan. Then, the data columns containing force, displacement, and gap height values were processed. For data manipulation, the force, displacement, and gap height data were first converted to a consistent unit system and sign convention. The gap height or force data were not further processed unless a systematic offset was identified in the recorded measurements. During code development, the data processing functions for individual participants were sanity-checked through blind comparison between sample force–gap height curves

manually plotted by each participant following a written version of the algorithm and the corresponding curves generated by the program.

Further data processing was performed to enable calculation of the mean and standard deviation across the six repeats for each testing and specimen configuration, as well as subsequent quantitative comparison among participants. Linear interpolation was applied to align all force–gap height data at common gap height values. Interpolation was performed using a uniform interval of 0.01 mm between the initial gap height of 11 mm and the final gap heights of 7 mm, 5 mm, and 3 mm. To ensure consistency across datasets, all interpolated data were cropped to the common upper and lower gap height limits defined by the maximum and minimum values observed across all repeats of the same testing and specimen configuration. The mean and standard deviation were then calculated at each interpolated gap height point to obtain the average response and variability of the datasets.

Flow front profiles. Flow front profiles were determined from 24-bit colour images downscaled to 8-bit greyscale images of all individual specimens. All images were obtained by the participants using flatbed scanners of their choice, with a fixed spatial resolution of 600 dpi. A ruler was placed adjacent to each specimen in every image to enable spatial calibration where a reference length of 200 mm corresponded to 1182 pixels, resulting in a conversion factor of 0.1691 mm/px.

A global binary inverse threshold was applied to each image using a threshold value of 254 to generate a binary mask. This threshold value was selected based on the assumption of a near-white background while allowing for minor scanner noise. Following thresholding, the specimen appeared as the foreground region in the binary mask. A rectangular region-of-interest (ROI) mask was then applied to restrict specimen detection to a known area, excluding scanner borders and edge artefacts near the image boundaries.

The flow front profile was determined using a contour-based edge detection approach. External contours were extracted from the binary mask and represented as ordered lists of pixel coordinates in a Cartesian x–y coordinate system with a resolution of one pixel. Among all detected contours, the longest contour (i.e., the contour containing the largest number of points) was selected as the flow front profile of the specimen.

A specimen centre was subsequently determined by computing the mean of all pixel coordinates along the extracted flow front profile. All flow front coordinates were then re-centred relative to this centre and converted from pixel units to physical dimensions in mm using the established conversion factor of 0.1691 mm/px.

To obtain a representative average flow front for specimens of the same type, individual flow front profiles were combined using a correspondence-based averaging approach. The shortest profile (i.e., the profile containing the smallest number of points) was selected as a reference. For each point on this reference profile, the closest points on all other specimen profiles were identified and then averaged to produce a representative mean flow front profile for the specimen type.

Results and Discussions

Variability in raw material. Figure 2 presents an overview of the experimentally measured thickness, density, and areal weight of the raw specimens. The data presented in Figure 2 were averaged across all participants and all specimens, including both 50 mm and 100 mm specimens. It can be observed that CF4012K exhibits the highest coefficient of variation (COV) in both thickness and areal weight, with values of 7.22% and 7.51%, respectively. For density, CF4012K shows a comparatively high COV of 6.03%, second only to CF503K, which exhibits a marginally higher density COV of 6.05%. Overall, the observed levels of variability (approximately 5–8%) are consistent with the ranges commonly reported for raw SMC materials in the literature [7]. In addition, the mean areal weights of all five materials lie within 5.88% of the target areal weight of 1800 g/m², which is generally regarded as very good consistency for this class of material.

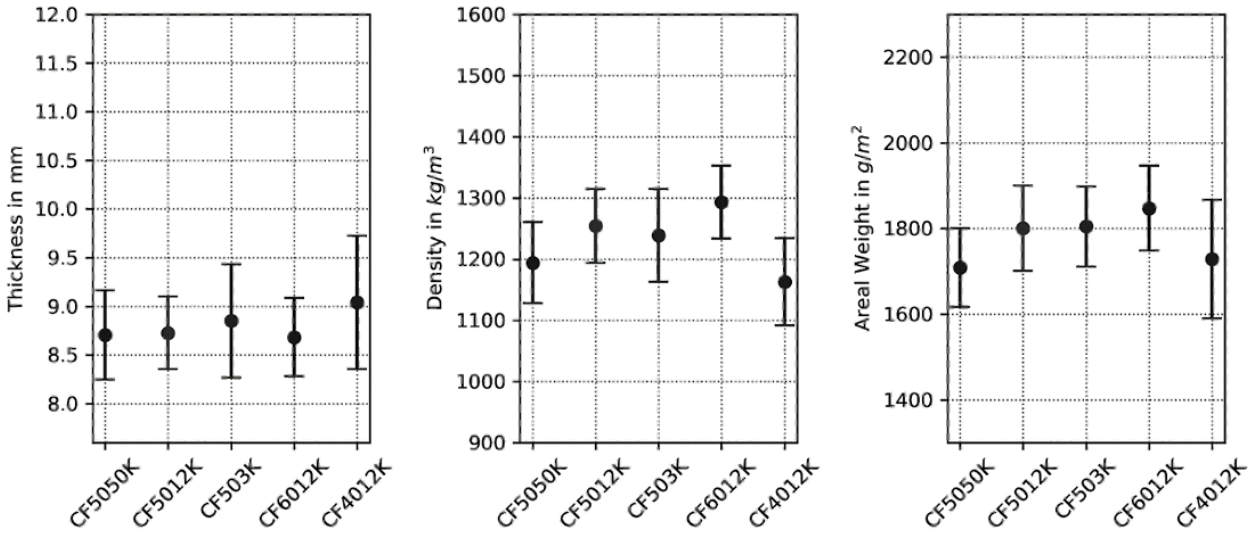

Fig. 2. Thickness, density and areal weight results for raw specimens. Data were averaged across all participants and specimens (including both 50 mm and 100 mm specimens)

It should be noted that the variations observed in the three quantities shown in Figure 2 can arise from different sources of material variability. Areal weight is primarily affected by the local fibre content and is therefore most strongly influenced by the fibre deposition stage of the SMC manufacturing process. During this stage, parameters such as tow cutting speed and carrier foil transport velocity must be carefully controlled to achieve the target areal weight. Maintaining such control becomes increasingly challenging for larger tow sizes or wider ranges of fibre content, particularly when using equipment optimised for a nominal fibre mass fraction of approximately 50% and a tow size of 12K. Thickness and density, on the other hand, are also affected by downstream impregnation and lay-up processes. Several authors have reported that raw SMC layups commonly exhibit increased apparent thickness due to trapped air and lofting effects between plies of non-uniform thickness. Apparent volume increases of up to approximately 20% have been reported for such materials [2, 7], which directly result in lower calculated densities prior to consolidation.

Force-gap height relationship. Figure 3 presents example force-gap height graphs of four out of the five materials tested in the 100 x 100 mm^2 specimen size configuration for the participants capable of testing this specimen size. The results show a high level of variation in the measured forces among participants despite the fact that a well-prescribed testing procedure was implemented. All curves show an increase in measured force with reducing gap height, with most curves exhibiting an initial steep slope, once contact has been established that levels off in the medium compression range, and then increases again near the end.

It should be noted that the force–gap height curves obtained by IVW exhibit a higher level of noise compared with those from the other participants, with negative forces observed at low levels of compression (gap heights greater than approximately 8 mm). This behaviour is likely attributable to the larger hydraulic press used by IVW, which may introduce greater inertia effects and structural vibration than the smaller-scale testing machines employed by the other participants. In addition, IVW used a load cell with a measurement range of 8000 kN, far exceeding the force levels recorded in the benchmark (below 100 kN). By comparison, the other participants selected load cells rated up to 250 kN. As a result, IVW's measurements were more susceptible to reduced accuracy at the low end of the measured force range.

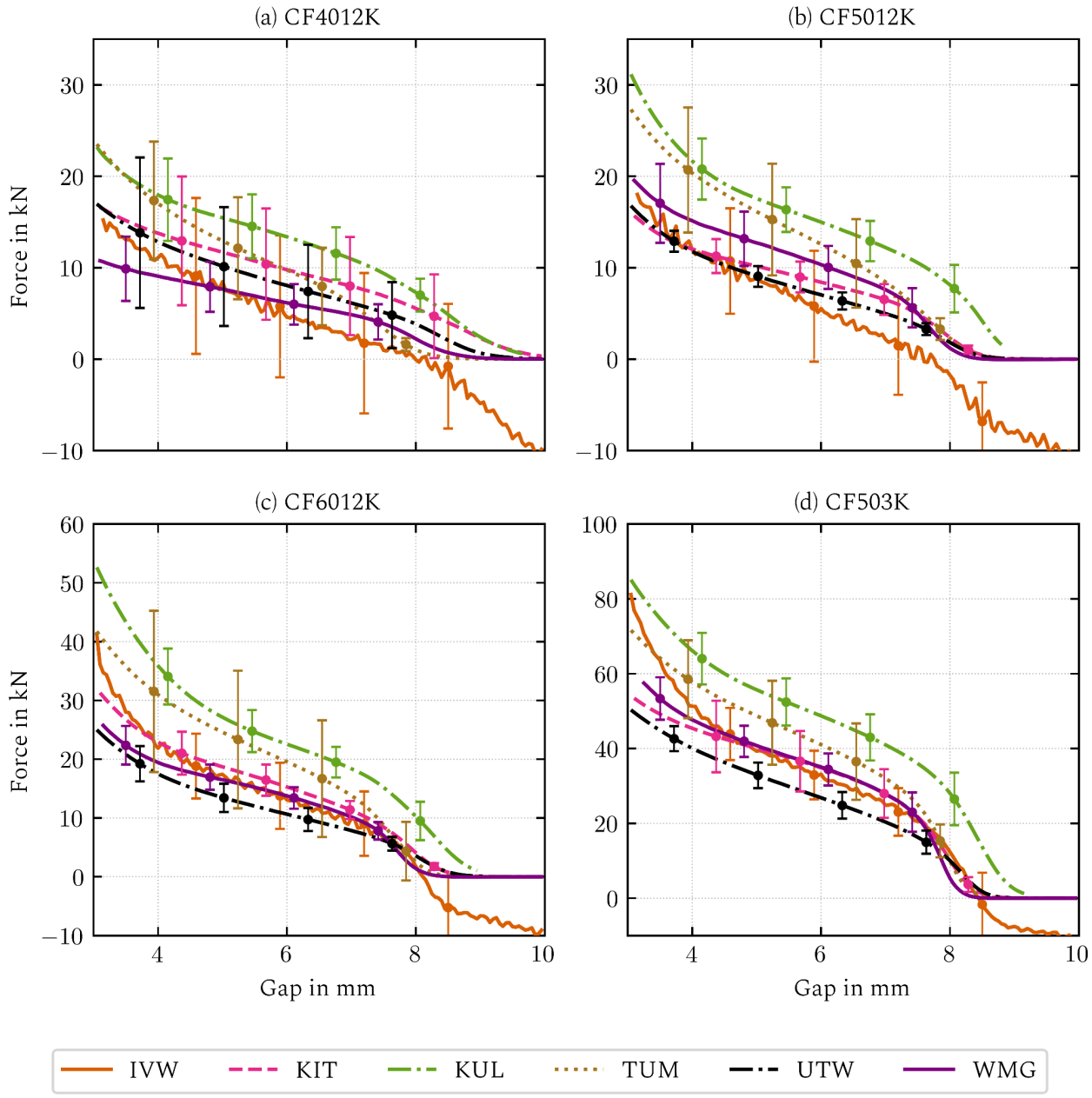

Fig. 3. Example force-gap height curves for four of the five materials in the 100 x 100 mm^2 specimen size configuration. For the purpose of clarification, only four data markers and corresponding error bars are displayed for each curve.

Figure 3a–c illustrate the effect of increasing fibre weight fraction from 40% to 60%. At low levels of compression (gap height of approximately 8 mm), the measured forces show no strong correlation with fibre content, with values typically ranging from 3 to 10 kN at a gap height of 8 mm across all participants. This behaviour is attributed to deformation mechanisms dominated by the removal of trapped air and lofting between plies, with negligible deformation of the fibre network. As a result, the compressive forces at this stage are largely independent of fibre content. At intermediate levels of compression (gap height of approximately 6 mm), no noticeable increase in force is observed as the fibre weight fraction increases from 40% to 50%. However, a substantial increase in force of approximately 50% is observed when the fibre weight fraction increases from 50% (approximately 5–15 kN) to 60% (approximately 10–25 kN) at a gap height of 6 mm. At high levels of compression (gap height of approximately 4 mm), the influence of fibre content becomes more pronounced. An increase in force of approximately 30% is observed as the fibre weight fraction increases from 40% (approximately 9–17 kN) to 50% (approximately 12–22 kN), followed by a further increase of approximately 60% as the fibre weight fraction increases to 60% (approximately 18–36 kN). In

addition, the standard deviation of the measured forces decreases with increasing fibre content, as indicated by the shorter error bars. In general, an increase in fibre content is expected to result in higher forces beyond the initial compression regime, after trapped air has been released or compressed. The higher force is attributed to increased fibre–fibre interactions and tow compaction, which lead to elevated shear and compressive stresses within the material. At higher levels of compression, this effect is expected to intensify, as internal stresses exhibit a nonlinear relationship with compression due to the progressive stiffening of the fibre network.

Figure 3b and 3d illustrate the effect of decreasing the tow size from 12K to 3K, for which a pronounced increase in force is observed across all levels of compression. At low levels of compression (gap height of approximately 8 mm), the measured force range increases by more than a factor of 3 as the tow size decreases from 12K (approximately 3–7 kN) to 3K (approximately 10–30 kN). At intermediate levels of compression (gap height of approximately 6 mm), the force increases by approximately a factor of 4, from around 7–15 kN for 12K to 30–50 kN for 3K. At high levels of compression (gap height of approximately 4 mm), the force increases by just over a factor of 2, from approximately 12–22 kN for 12K to 40–70 kN for 3K. No noticeable difference in the level of standard deviation is observed between the two tow sizes. In theory, for a given fibre content, reducing tow size increases the number of tows within the same volume of material, leading to higher levels of fibre–fibre interaction and consequently, an accelerated increase in force with increasing compression. This effect is expected to dominate primarily beyond the initial compression stage, once trapped air has been fully removed. While the data presented in Figure 3 do not fully substantiate this assumption, the current analysis is limited to a qualitative assessment based on overall force ranges across all participants. Further in-depth analyses will be conducted with a focus on the detailed trends of individual force–gap height curves for each participant.

As discussed in the Introduction, the observed variability in the results can be attributed to a range of factors. For example, some participants (IVW, JKU, WMG) employed presses or testing frames with hydraulic drives, while others (UOB, KUL, KIT, UTW) used screw-driven electromechanical testing machines. These differences can lead to variations in testing control accuracy, as electromechanical drives generally provide more precise displacement control within the speed range adopted in this benchmark, while hydraulic drives may exhibit greater speed fluctuations under these conditions. The specific implications of IVW's large press size and load cell capacity on the measured force signals have also been discussed earlier in this section. In addition, the type of heating system varied among participants. Some facilities employed self-heated platens with cartridge or fluid-based heating, whereas others used convection heating within an environmental chamber. These differences can lead to substantial variations in the steady-state temperature distribution at the tooling surfaces, while the use of an environmental chamber may introduce additional temperature fluctuations during specimen loading and unloading. The most critical sources of variability have therefore been categorised into testing procedure, testing equipment, and material related factors, as summarised in Table 2.

Table 2. Parameters considered in the statistical analysis.

Category	Parameters	Typical values/range
Testing procedure	Specimen loading time	10-30 s
	Release agent	Loctite-frekote-700NC Marbocote 227 CE Chemlease PMR 90
Testing equipment	Machine type	Electromechanical testing frame Hydraulic testing frame Hydraulic press
	Heating method	Environmental chamber Heated platens
	Load cell range	50-8000 kN
	Displacement measurement	Video extensometer/Optical Crosshead displacement LVDT
Material Specimen	Environmental conditions	Temperature 15-19 °C Humidity 33%-76%
	Material location	(Specific labelling system for roll and batch tracking)
	Testing dates	22 October 2024 – 28 November 2024
	Specimen size	50 x 50 mm^2 100 x 100 mm^2

Flow front profiles. Figure 4 shows the processed flow front profile data for the same four example materials shown in Figure 3. It should be noted that with the current method, the centre of each flow front profile was calculated as the mathematical averaging of all the x-y coordinates on the profile, which is not necessarily aligned with the true specimen centre, as the flow might not be symmetrical due to factors such as mould tilting and material heterogeneity. This approach was adopted due to the lack of reference marking of the specimen centre, which is a shortfall that should be addressed in future squeeze flow testing.

It can be seen in Figure 4 that at the final gap height of 3 mm, CF503K exhibits the shortest flow distances, where the shape of the flow front profile also shows the smallest deviation from the original square specimen shape. CF4012K on the other hand shows the longest flow distances as well as largest deviation from the original square specimen shape. The observed difference in flow distances between corresponds well to the force data, where CF503K and CF4012K exhibited the highest and lowest forces respectively to reach the 3 mm final gap height due to a combined effect of fibre content and tow size as discussed in the force-gap height section.

For the CF503K and CF4012K materials, there is also a noticeable discrepancy in the level of variation among participants. This noticeable discrepancy suggests that the variations in testing procedure and testing equipment among participants is likely to amplify the effects of material variations. Other than the clear outlier (TUM) for CF503K, CF503K and CF6012K show the lowest level of variations both within and among participants. Analogous to the force curves, the CF4012K and CF5012K exhibit higher levels of variations both within and among the participants than CF6012K and CF503K. It can therefore be considered that C-SMC materials with higher fibre content and smaller tow size tend to be less sensitive to the variability in testing procedure and testing equipment. It is interesting to note that such materials tend to provide better mechanical properties such as stiffness and strength, although at a higher material cost.

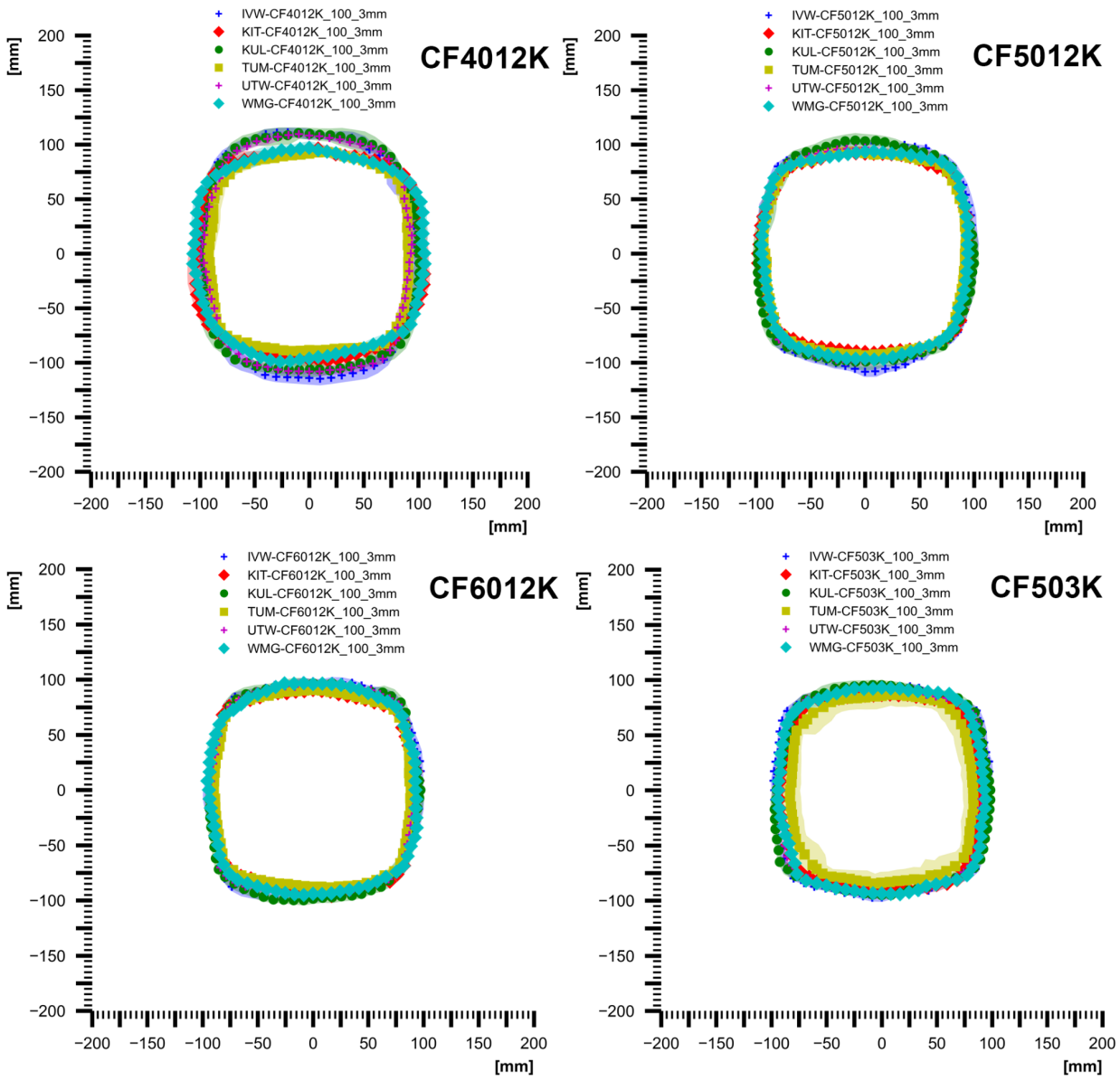

Fig. 4. Example flow front profiles extracted from four of the five materials with 100 x 100 mm^2 specimen size configuration.

Conclusion and Future Work

Initial data processing has been conducted to provide an initial quantitative overview of the experimental results, including variability in the raw material, force–gap height relationships, and flow front profiles. The levels of variability observed in the raw material, in terms of specimen thickness, density, and areal weight, are consistent with those reported in the literature. Preliminary assessment of the force–gap height curves indicates that material parameters such as fibre content and tow size have a strong influence on the compressive forces once the material has passed the initial compression stage, during which trapped air is fully removed. Specifically, the measured forces increase with increasing fibre content and decreasing tow size, which is attributed to enhanced fibre–fibre interactions. Analysis of the flow front profiles suggests that materials requiring higher compressive forces—such as those with higher fibre contents and smaller tow sizes—tend to exhibit shorter flow distances under the same compression displacement and show reduced deviation from the original square specimen geometry. Variations observed in both the force–gap height relationships and flow front profiles can be attributed to a combination of factors related to the testing procedure, testing equipment, and material or specimen parameters. In general, materials with lower fibre

contents and larger tow sizes appear less sensitive to variability arising from differences in testing procedure and equipment.

The next phase of the study will focus on a more comprehensive and quantitative evaluation of the collected dataset. Statistical analyses are currently being performed to quantify variability in the processed force–gap height relationships and flow front profiles, and to identify correlations between the factors summarised in Table 2 and the observed variability. This analysis will assess repeatability and reproducibility within and across participants, evaluate the consistency of mean responses, and distinguish the relative contributions of the different sources of variability.

The outcomes of this benchmark exercise will support the development of a robust testing procedure and associated guidance for squeeze flow testing of high-performance C-SMCs, and will contribute towards the standardisation of this testing method. In addition, these efforts aim to improve the reliability of flow-modelling input data for C-SMC composite part manufacturing simulations.

Acknowledgement

The authors thank Polynt Composites Germany GmbH for their generous donation of all the materials used in this benchmark exercise.

References

[1] Romanenko, V., et al., Advanced process simulation of compression molded carbon fiber sheet molding compound (C-SMC) parts in automotive series applications. Composites Part A: Applied Science and Manufacturing, 2022. 157: p. 106924.

[2] Yuan, H., et al., Experimental process characterisation for high-volume compression moulding of hybrid-architecture composites. Composites Part A: Applied Science and Manufacturing, 2024. 181: p. 108137.

[3] Mahé, F., et al., A revisited compression flow model for concentrated suspensions with fiber-friction interactions. Journal of Non-Newtonian Fluid Mechanics, 2023. 319: p. 105090.

[4] Schreyer, L., et al., Characterization and modeling of the anisotropic flow behavior of long carbon fiber reinforced thermoplastic compression molding. Composites Part A: Applied Science and Manufacturing, 2025. 198: p. 109053.

[5] Kapshammer, A., et al., An Advanced Compression Molding Simulation and Validation of a Thick-Walled Carbon Fiber Sheet Molding Compound Brake Caliper. Journal of Manufacturing and Materials Processing, 2025. 9(4): p. 137.

[6] Qian, C., et al., The first European benchmark exercise on squeeze flow testing of high-performance carbon fibre sheet moulding compounds. 2025. 676–685.

[7] Schommer, D.M., Charakterisierung und Modellierung des Materialverhaltens von kohlenstofffaserverstärkten Sheet Molding Compounds während des Fließpressens. 2025, Leibniz-Institut für Verbundwerkstoffe GmbH: Kaiserslautern.

The publication of this article was funded by the KU Leuven 10.13039/501100004040